

Implementation of a Real-time Differential Path-length Spectrometer System

T. P. Moffitt and S. A. Prahl
BME Dept., Oregon Health & Science
University, Portland, OR

ABSTRACT

We report on the development of an optical-fiber-based diagnostic instrument to determine the local optical properties of a turbid media. The system relies on making differential diffuse reflection measurements. We present a method to correct for the variations in the spectral characteristics of the two spectrometers. We also introduce a novel method to evaluate the differential reflectance by encoding a relative wavelength sensitivity constant into the signal processing to account for differences in the spectral sensitivity between spectrometers. This method allows us to record differential reflectance without needing to make additional reference measurements before an experiment to account for spectral variation of the lamp.

keywords: tissue, reflectance, scattering, absorption.

1. INTRODUCTION

Determining the optical scattering and absorption properties of tissue for diagnostic and therapeutic applications is of interest in medicine. Most reflectance techniques rely on light distribution information over a large area ($>1 \text{ cm}^2$) and use separate illumination and collection fibers with a separation distance of several millimeters¹ or have mixed fiber bundles with source and emission fibers randomly arranged from 0.1-1 mm from each other.²

Two studies on devices with separate source and detector fibers show that the mean photon penetration depth increases as the square root of the separation between source and detector fibers either spatially³ or temporally.⁴ Source-detector fiber devices sample relatively large volumes, because of the separation between the fibers.^{3,4} Though effort has been made to minimize the sampling volume using small source-detector separations,⁵ little work has been done on photon penetration depths when the source fiber is also used to collect backscattered photons.⁶ Since large sampling volumes are less likely to be homogenous, we are developing a device that acquires information from small volumes of tissue ($< 1 \text{ mm}^3$) by using the same fiber for both source and detector.

A recent technique introduced by Amelink et al.⁷ that uses small collection volumes is differential path-length spectroscopy (DPS). We encountered a couple of issues that are inherent in using two separate spectrometers. The two spectrometers differ slightly in their respective wavelength scales and also differ in their spectral sensitivities. We use a different normalization method than Amelink which requires correction factors that are not encountered by Amelink's method. We show that for our system, a stepping function to shift the wavelength bin of one spectrometer channel to the other can be established from a linear fit for bin shifting. We also describe a method to process data rapidly that corrects for the difference in spectral sensitivity between spectrometers using a relative wavelength sensitivity constant.

Further author information: (Send correspondence to S.A.P.)
S.A.P.: E-mail: prahl@bme.ogi.edu, Telephone: (503) 216-2197, 9205 SW Barnes Rd., Portland, OR 97006, USA

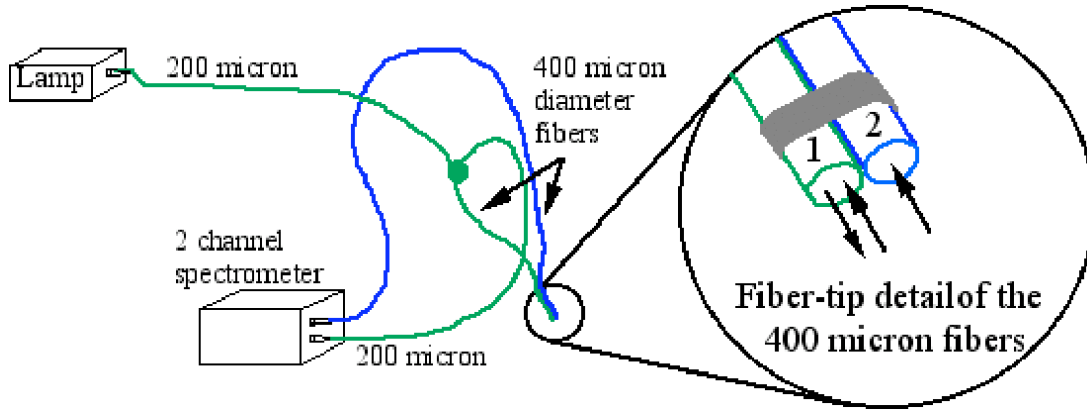


Figure 1. The experimental set-up consists of two 400 micron fibers that are fixed together at the end used for light collection. A dual channel spectrometer collects the two signals sequentially with a minimum 22 ms integration time. For the differential path-length spectroscopic system as shown, one of the the fibers is bifurcated by end-coupling two 200 micron diameter fibers to a single 400 micron diameter for illumination and collection. Since we were evaluating the performance of the two detectors channels of the spectrometer the 200 micron bifurcation fibers were removed and both 400 micron fibers were connected directly to the spectrometers.

2. MATERIALS AND METHODS

A differential path-length spectrometer system is constructed based on the design of Amelink et al.⁸ The system is a fiber-based diffuse reflection spectrometer using an Ocean Optics Dual channel spectrometer as a detector (SD2000, Ocean Optics Inc., Dunedin, FL) with a tungsten-halogen lamp (LS-1, Ocean Optics Inc., Dunedin, FL) as a white light source. The DPS apparatus is shown in figure 1. The first spectrometer uses a bifurcated fiber by end-coupling with SMA connectors two identical 200 micron diameter fibers to a single 400 micron diameter fiber at the probe end for illumination and collection. A second 400 micron diameter fiber carries diffusely reflected light to a second spectrometer. The two 400 micron fibers were fixed together near the collection faces using heat shrink tubing. For the special case of evaluating differences in the spectrometers, the 200 micron bifurcation fibers were removed and the 400 micron fiber was directly connected to the first spectrometer so that it only collects light.

The spectrometer is interfaced to a laptop computer using LabView Software (National Instruments) in conjunction with a DAQcard-700 (National Instruments) PCMCIA card. The software interface displays the reflectance spectrum of each spectrometer continuously with independent adjustable integration times (minimum is 22 ms). The spectra are recorded sequentially for the first and second spectrometers.

Each spectrometer recorded a spectrum with a slightly different wavelength scale. The wavelength depends upon the grating alignment and relates each wavelength to a particular pixel on the CCD. In each spectrometer, the wavelength scale was described by the manufacturer using a second order polynomial. Spectra were recorded of three known wavelength sources: a green He-Ne laser (543.5 nm), a red He-Ne laser (632.8 nm) and a near-infrared diode laser (795.2 nm). Each spectrometer collects light in 2048 wavelength bins. The peaks are normalized with the maximum equal to 1 for comparison by shifting the wavelength bins of the first spectrometer relative to the second. The difference was taken between the first and the shifted second spectrometer allows correlation of the bins of the two spectrometers.

The two spectrometers have differing spectral sensitivities. Two identical 400 micron fibers were connected to each spectrometer. Spectra were recorded using several diffuse light source arrangements. The fibers were positioned facing a glass diffuser that was illuminated from the opposite side. The illumination spot was concentric with the collection fibers and had a diameter of illumination greater than the cone of acceptance for the fibers. Three light source arrangements were used: a tungsten lamp (Ocean Optics LS-1), a variable power tungsten lamp (Fiber-Lite illuminator) or natural light from the sky. The variable tungsten lamp power was

varied to get a strong signal from 400 to 500 nm (sacrificing signal at longer wavelengths due to saturation) and from 500 to 900 nm. Another experimental arrangement used the same lamps but aimed onto a 99% Spectralon reflectance standard (Labsphere, Inc.). The collection fibers were held a fixed distance and perpendicular to the Spectralon standard surface with the incident light delivered through a 600 micron fiber positioned in-line and in contact to the collection fibers. Finally, light from the sky (without clouds) was recorded by simply aiming the optical fibers out a window.

The spectra collected in the above experiments were used to create a wavelength dependent scaling factor, $\alpha(\lambda)$, to correct for the differences in spectral sensitivity between the two spectrometers. The correction factor, $\alpha(\lambda)$, was derived using the ratio of the first spectrometer to the second spectrometer. This ratio was evaluated for each of the above diffuse light source measurements. Any variance between ratios $\alpha(\lambda)$ for different sources could be eliminated solely by a single multiplicative constant. All ratios were arbitrarily scaled to be equivalent to the tungsten lamp measured in transmission through the glass diffuser (without any room-light contribution). That particular ratio was selected because the tungsten lamp would be used in the DPS system.

After scaling, the average ratio was calculated using a combination of all the spectra with different wavelength ranges. Spectra ranges were limited either due to saturation of the detectors or by a poor signal to noise ratio. Scaling was achieved by ensuring the spectral ranges for the various measurements overlap. Finally, a 15 element window average which corresponds to a 5 nm bandwidth window was taken across the entire spectrum of α to smooth out noise. The window average was repeated an additional two iterations.

The overall average of all these measurements is $\alpha(\lambda)$. A fiber connected to the first spectrometer was replaced with a bifurcated fiber composed of two 200 micron fibers end-coupled to another 400 micron fiber as shown in figure 1. The green fiber in figure 1 can then both illuminate and collect light while the blue fiber only collects light. The fibers were placed on the surface of a fresh porcine liver obtained from a supermarket .

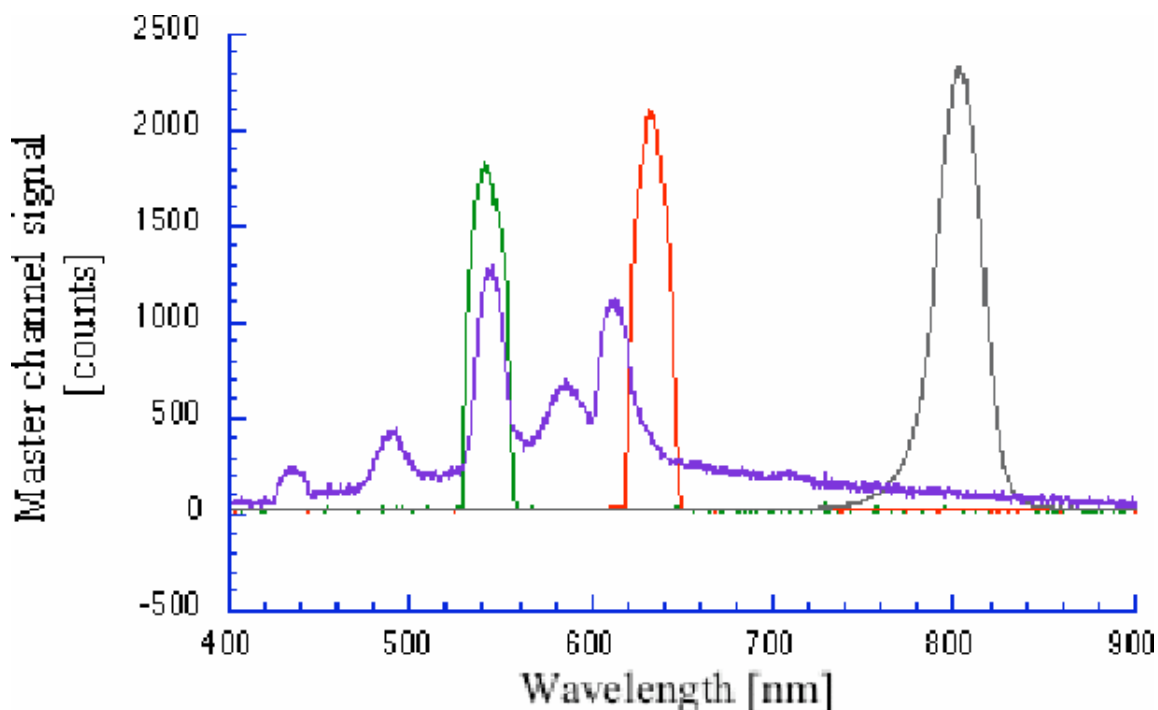


Figure 2. Typical spectra for the three lasers in transmittance through a glass diffuser and a spectra of the room and fluorescent lights reflected off a 99% Spectralon standard. The peaks of the fluorescent lamp were determined using an optical fiber coupled to a Fluorolog-3 fluorimeter detector.

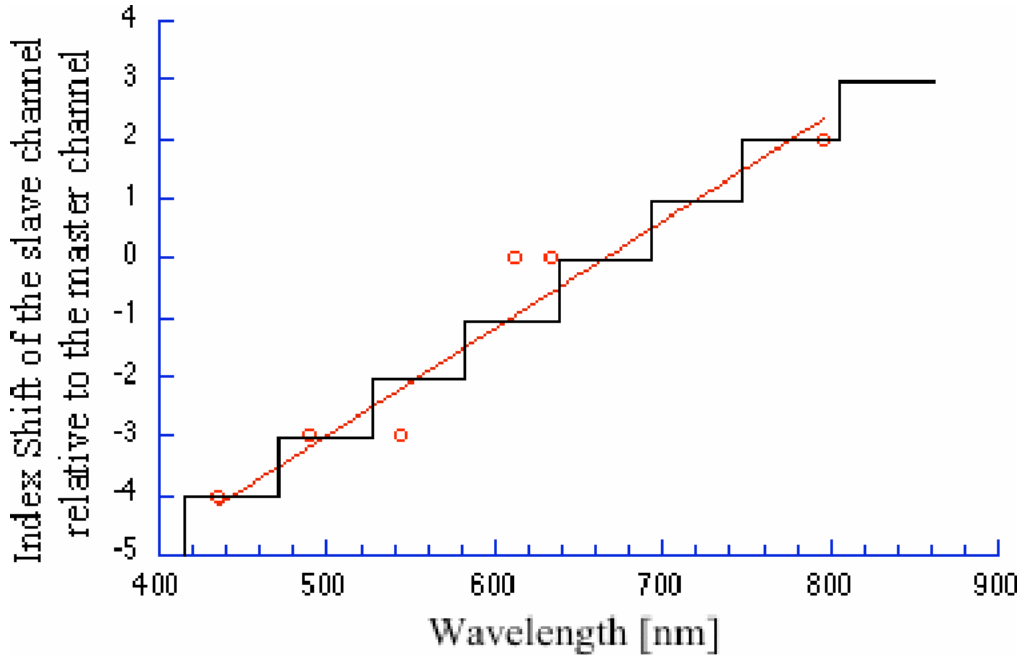


Figure 3. The optimal bin shift for the slave channel relative to the master channel using the peaks from fluorescent room lights, green and red He-Ne lasers, and a near-infrared diode laser. The red line is a linear fit to the discrete shifts in bins and is used to denote the wavelength corresponding to a bin where the shifts step to the next discrete value shown by the black stepping function and occur at 408.0, 461.8, 515.7, 569.5, 623.3, 677.1, 731.0, and 784.8 nm.

The data processing algorithm to produce the differential reflectance, R_{diff} was as follows:

$$R_{\text{diff}} = \frac{R_1 - \alpha(\lambda)R_2}{R_1}$$

where R_1 and R_2 are the spectra from the first and second spectrometers respectively, $\alpha(\lambda)$ is a spectra constant that correlates the difference in spectral sensitivity between the two channels. Three spectra were recorded, the differential reflectance and spectrum of each spectrometer.

3. RESULTS

Spectra for the three laser sources and the overhead fluorescent lights are shown in Figure 2 for one spectrometer. The wavelength bin of the second spectrometer were shifted and subtracted from the first to find the minimum difference between channels (after peak normalization). In figure 3, the number of bins that the second is shifted relative to the first spectrometer is plotted versus the wavelengths of the peaks. A linear fit determined the wavelength bin for the stepping the index shift. The resultant difference after shifting is shown in figure 4. The absolute error for each laser wavelength was calculated across the width of the peak which is shown in Table 1.

The raw ratios of the first to the second spectrometer is shown in figures 5 and 6. The scaled spectra are shown in figure 7 in addition to the smoothed wavelength correction factor $\alpha(\lambda)$.

4. DISCUSSION

We chose a different method than Amelink et al. to normalize our DPS spectra. Amelink's normalization takes the following form:

$$R_{\text{diff}} = \frac{R_1}{R_{1,\text{back}}} - \frac{R_2}{R_{2,\text{back}}}$$

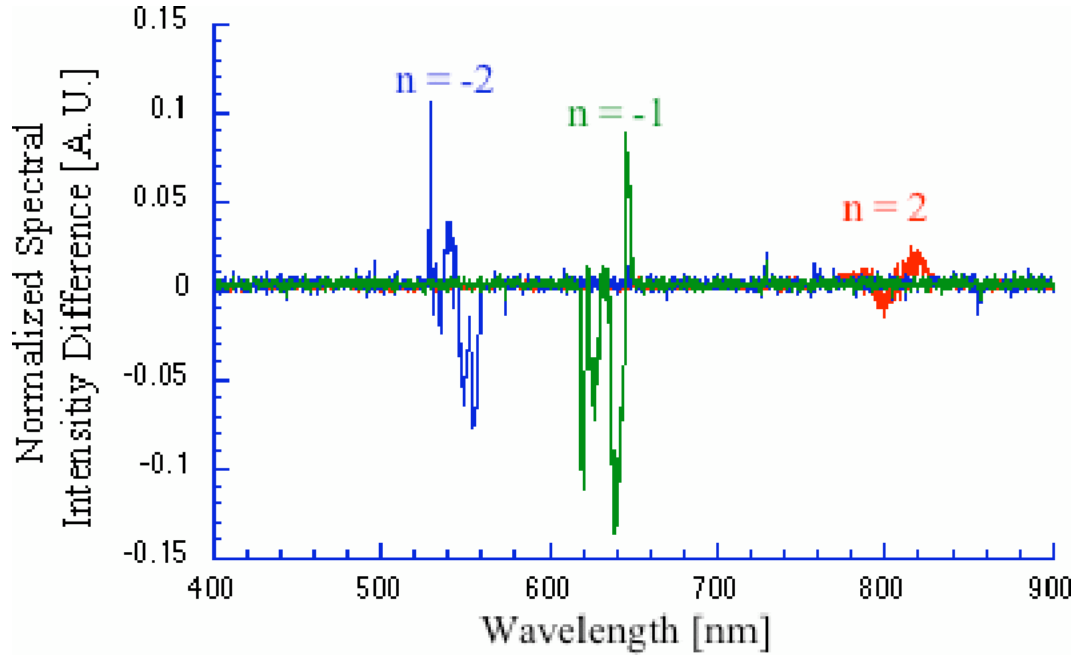


Figure 4. The difference of the the normalized peaks between spectrometer channels is shown relative to the noise floor for each laser source. These differences are the result of bin shifting.

bin shift (nm)	528–560 nm	617–653 nm	760–840 nm
+3	—	—	0.69%
+2	—	6.0%	0.55%
+1	—	4.5%	1.0%
0	6.6%	3.8%	1.8%
-1	4.6%	4.3%	2.5%
-2	2.9%	5.2%	3.3%
-3	2.3%	6.4%	4.0%
-4	3.1%	7.6%	4.8%
-5	4.7%	—	—

Table 1. The absolute error that remains as a percentage of the spectral peak is given for a 543.5 nm He-Ne, a 632.8 nm He-Ne and a 795.2 nm Diode laser for the given wavelength bin shift. Each channel of the spectrometer requires a different wavelength scale for the 2048 bins of the linear CCD. The data in this table shows the degree to which the error between spectrometer channels changes from shifts in bin indexing.

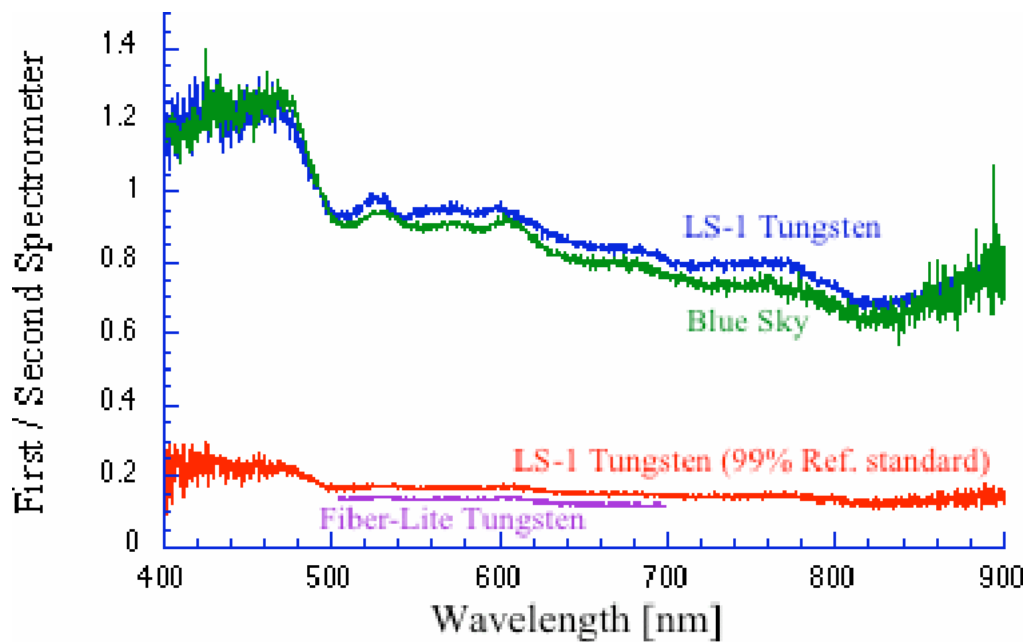


Figure 5. The ratio of the master channel to the slave channel for identical light collection arrangements. The sky was measured by aiming the collection fibers out a north window. Two different tungsten lamp are measured either in transmission through a white glass diffuser or in reflection off a 99% reflection standard.

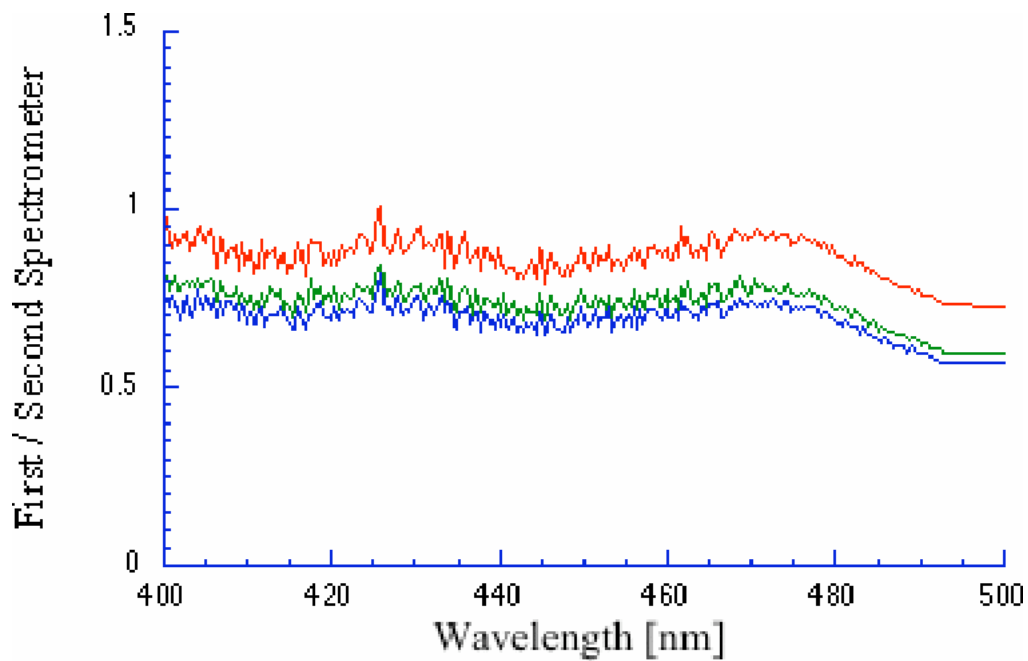


Figure 6. To reduce noise between 400 and 500 nm, the output power of a variable intensity tungsten lamp was increased at the cost of detector saturation above 500 nm. Again the ratio of the master channel to the slave channel is shown optimized for wavelengths below 500 nm.

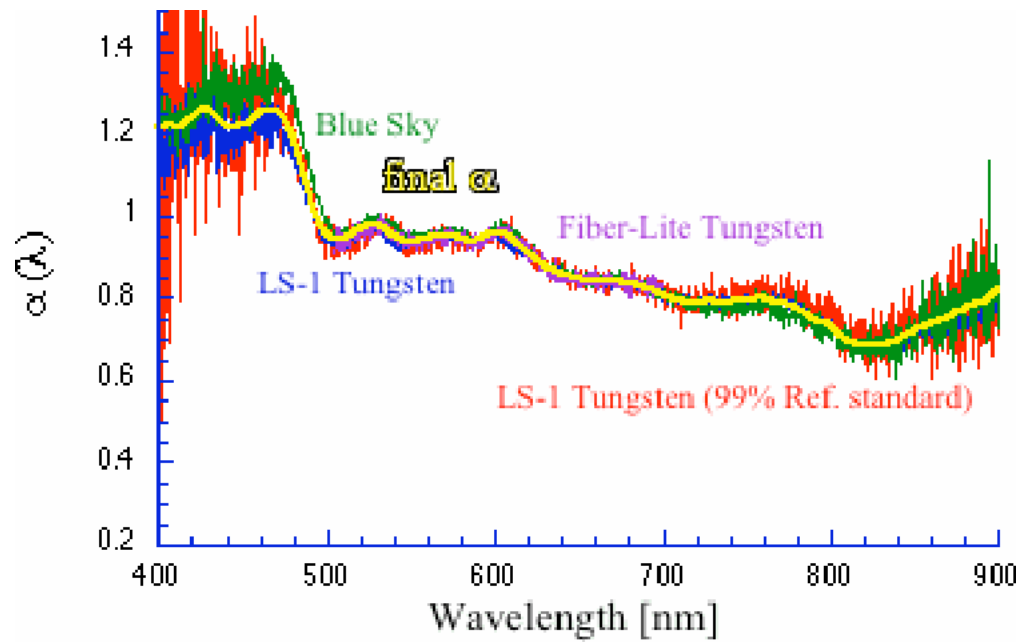


Figure 7. The relative spectral sensitivity function, α (yellow) is a combination of the scaled ratios of the master to slave channel. The α curve is smoothed using a 5 nm band window average.

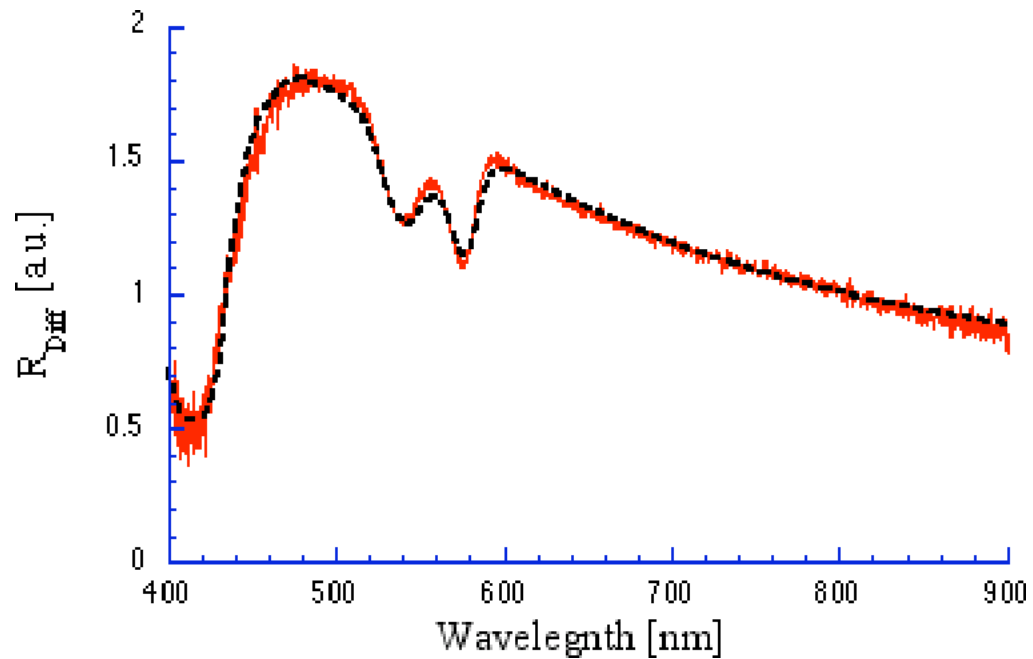


Figure 8. The corrected differential reflectance obtained from an *in vivo* porcine liver surface. The dashed line is a fit using the absorption spectra of hemoglobin.

where R_1 and R_2 are the raw respective spectra for the measured sample and $R_{1,\text{back}}$ and $R_{2,\text{back}}$ are the spectral measurements of a standard reference such as a Spectralon standard. The equation can be rewritten

$$R_{\text{diff}} = \frac{R_1 - \left(\frac{R_{1,\text{back}}}{R_{2,\text{back}}}\right) R_2}{R_{1,\text{back}}}$$

Our normalization is given by

$$R_{\text{diff}} = \frac{R_1 - \alpha(\lambda)R_2}{R_1} = 1 - \alpha(\lambda)\frac{R_2}{R_1}$$

Since we defined $\alpha(\lambda) = \frac{R_{1,\text{back}}}{R_{2,\text{back}}}$, our normalization is nearly identical excepting that our proposed normalization is scaled by the reflectance using the first spectrometer of the sample being measured and not of a standard reference measurement. The advantage being that the reference measurements for the two spectrometers are stored in the software and do not need to be repeated prior to an experiment to compare data from separate experiments.

A more complicated problem is correlating the wavelength ranges between the two spectrometers. Since the wavelength scales are described by quadratic equations, presumably the difference between scaled should also have a quadratic form. We found that across the visible spectrum, a linear correlation is sufficient but not perfect. A better correlation solution would be to take the output spectra of each channel separately and interpolate the data at defined wavelength intervals. The interpolated data spectra could then be processed as above to get at the reflection difference signal. In figure 3, the linear fit did not change if the fluorescent room light data peaks were omitted and the laser peaks alone are used to evaluate the stepping function. The shape of the error between spectrometer channels (figure 4) is not uniform across the spectra having a “W” shape in the blue through red but more of an “N” shape in the near infrared. This may be indicative of one of two details. First, current may be leaking from one CCD pixel to the next when a large gradient in the intensity occurs between pixels. The two spectrometers almost certainly leak current between pixels at different rates. Second, the spectrometers are designed to use a 200 micron slit as an aperture or the diameter of the fiber whichever is smaller. Slight differences in aperture width could affect the spread of a sharp spectral peak across a wider wavelength range. It must also be noted that the diode laser has a FWHM of 23 nm whereas the He-Ne lasers have much sharper spectral peaks and their spreading are certainly due to current leaking from one CCD pixel to the next.

Amelink et al. demonstrated that the reflection difference can be approximated by the relation

$$R_{\text{diff}} = \mu_s(\lambda_0) \left(\frac{\lambda}{\lambda_0}\right)^{-B} e^{-C\mu_a(\lambda)} + D$$

where $\mu_s(\lambda_0)$ is the reduced scattering coefficient at λ_0 , B the scattering wavelength dependence, C is a scaling factor related to the size of the collection fibers and D is an offset. The absorption coefficient, μ_a can be fit using a composite of the known chromophore absorption spectra. Using our method determining R_{diff} , we tested for the same behavior using the wavelength dependent absorption coefficient as given by

$$\mu_a(\lambda) = C_{Hb}(SaO_2\mu_a^{HbO_2}(\lambda) + (1 - SaO_2)\mu_a^{Hb}(\lambda)) + F_{H_2O}\mu_a^{H_2O}(\lambda)$$

Matlab is used to perform the fitting routine which returned the scalar values for the hemoglobin concentration (C_{Hb} [g Hb/l]), the oxygen saturation (SaO_2), the fraction of water (F_{H_2O}), $\mu_s(\lambda_0)$, B, C, and D. Our fit in figure 8, returned an oxygen saturation of 99.6% at a concentration of 76 g Hb/l and a water fraction of 35%.

We have presented a detailed description of the steps needed to fine tune a differential pathlength spectrometer system. We demonstrated that signals can be normalized by measuring the relative wavelength sensitivity constant $\alpha(\lambda)$. In addition, we demonstrated a method to correlate the wavelength scales of two separate spectrometers using a bin index stepping function based on a linear fit optimized by minimizing the absolute error between spectrometers. Our system exhibited common mode rejection at worst 4.3% around 633 nm and less than 1% around 795 nm with our corrections. We showed that our signal processing method behaves in an

equivalent fashion to the method of Amelink et al. Though the elements of differential path-length spectrometer system are few and fairly inexpensive, the system works well in the challenging task of evaluating tissue optical properties in small sampling volumes.

Acknowledgements

This work was funded by a grant from the National Institutes of Health: NIH-CI-R24-CA84587-04.

REFERENCES

1. M. G. Nichols, E. L. Hull, and T. H. Foster, "Design and testing of a white-light, steady-state diffuse reflectance spectrometer for determination of optical properties in highly scattering systems," *Appl. Opt.*, **vol. 36**, pp. 93–104, 1997.
2. N. Kollias95, "The physical basis of skin color and its evaluation," *Clinics in dermatology*, **vol. 13**, pp. 361–367, 1995.
3. G. H. Weiss, R. Nossal, and W. F. Bonner, "Statistics of penetration depth of photons re-emitted from irradiated tissue," *J. Modern Optics*, **vol. 36**, pp. 349–359, 1989.
4. M. S. Patterson, S. Anderson-Engels, B. C. Wilson, and E. K. Osei, "Absorption spectroscopy in tissue-simulating materials: a theoretical and experimental study of photon paths," *Appl. Opt.*, **vol. 34**, pp. 22–30, 1995.
5. F. Bevilacqua, D. Piquet, P. Marquet, J. D. Gross, B. J. Tromberg, and C. Despeursinge, "*In vivo* local determination of tissue optical properties: applications to the human brain," *Appl. Opt.*, **vol. 38**, pp. 4939–4950, 1999.
6. S. A. Prahl and S. L. Jacques, "Sized-fiber spectroscopy," in *SPIE Proceedings of Laser Tissue Interaction IX*, S. L. Jacques, Ed., vol. 3254, pp. 348–352, SPIE, Bellingham, 1998.
7. A. Amelink, H. J. Sterenborg, P. L. Martin, and S. A. Burgers, "In vivo measurement of the local optical properties of tissue by use of differential path-length spectroscopy," *Opt Lett.*, **vol. 29**, pp. 1087–1089, 2004.
8. A. Amelink and H. J. Sterenborg, "Measurement of the local optical properties of turbid media by differential path-length spectroscopy," *Appl Opt.*, **vol. 43**, pp. 3048–3054, 2004.